Crystallization Behavior of Poly(ethylene terephthalate)/ Multiwalled Carbon Nanotubes Composites

Guangjun Hu,[1,2] Xiyan Feng,[1,2] Shimin Zhang,[1] Mingshu Yang[1]

[1]*Beijing National Laboratory for Molecular Science (BNLMS), Key Laboratory of Engineering Plastics, Joint Laboratory of Polymer Science and Materials, Institute of Chemistry, Chinese Academy of Sciences, Beijing 100080, People's Republic of China*
[2]*Graduate School of Chinese Academy of Sciences, Beijing 100039, People's Republic of China*

Received 20 December 2006; accepted 29 December 2007
DOI 10.1002/app.28048
Published online 19 March 2008 in Wiley InterScience (www.interscience.wiley.com).

ABSTRACT: Crystallization behavior of poly(ethylene terephthalate)/multiwalled carbon nanotubes (PET/MWNTs) composites have been investigated under isothermal conditions and in comparison with the conventional nucleating agents, sodium benzoate, and micrometric carbon/glass fibers. In the PET/MWNTs composites, MWNTs promote the crystallization of PET as a heterogeneous nucleating agent, and the nucleation efficiency is greatly enhanced when MWNTs was homogeneously dispersed in PET matrix. In comparison with pure PET, spherulites size of PET/MWNTs composites is significantly reduced, and the shape becomes quite irregular. TEM images indicate that MWNTs bundles locate in the center of spherulites of PET and act as nuclei. Fold surface free energy during nucleation process for MWNTs nucleated PET is just half of pure PET, suggesting that MWNTs are efficient nucleating agents for PET. The sequence of nucleating ability of is given as follows: sodium benzoate>MWNTs>talc>carbon fibers≈glass fibers. The nucleation in the presence of sodium benzoate is a chemical nucleation process that may cause severe degradation of PET, but MWNTs nucleate PET through ''particle effect,'' which does not affect the molecular weight of PET. © 2008 Wiley Periodicals, Inc. J Appl Polym Sci 108: 4080–4089, 2008

Key words: carbon nanotubes; polyesters; crystallization; differential scanning calorimetry (DSC); nucleation

INTRODUCTION

Because of their extraordinary mechanical, electrical, and thermal properties, carbon nanotubes (CNTs) including single-walled carbon nanotubes (SWNTs) and multiwalled carbon nanotubes (MWNTs) have been recognized as next-generation filler for polymers. CNTs possess modulus of 10–1500 GPa, aspect ratio of 100–1000, thermal conductivity could be twice as high as that of diamond, and their electric-current-carrying ability could be as high as 1000 times of that for copper wires.[1] Several methods have been applied to prepare polymer/CNTs composites, including melt compounding,[2–6] solution compouding,[7–9] *in situ* polymerization,[10,11] latex fabrication,[12] and solid-state mechanochemical pulverization.[13] The properties of polymer/CNTs composites strongly depend on the intrinsic properties of CNTs and polymer matrix, CNTs dispersion state and alignment, and interfacial interaction between polymer and CNTs.

Correspondence to: M. S. Yang (yms@iccas.ac.cn).
Contract grant sponsor: Natural Science Foundation of China; contract grant numbers: 50473054 and 50533070.

Poly(ethylene terephthalate) (PET) has been extensively studied because of the academic and commercial importance of this polyester.[14–16] Its unique molecular structure endues PET with a high glass-transition temperature and a slow crystallization rate. To achieve appropriate degree of crystallinity, a large number of heterogeneous nucleating additives such as sodium benzoate, talc, and titanium dioxide have been attempted.[17–20]

In the previous work,[21] we have prepared PET/MWNTs composites with low percolation thresholds of electrical conductivity and rheology by coagulation method. We find that interfacial interactions exist between PET and MWNTs, which could be a basis for soft epitaxy of PET crystallization. Furthermore, MWNTs are uniformly dispersed throughout PET matrix, which is conducive to achieve high nucleation density. These findings inspire us to consider the potential nucleation of PET by MWNTs. We have also noticed that there are some literatures that concentrate on the nucleation of CNTs on polymers.[22–24] In this study, crystallization behavior of PET/MWNTs composites have been investigated with polarizing optical microscopy (POM), transmission electron microscopy (TEM), and differential scanning calorimetry (DSC). The influence of MWNTs dispersion state on the crystallization

behavior of polymer matrix was investigated with two kinds of PET/MWNTs composites prepared from different methods. Crystallization behavior of PET/MWNTs composites have been investigated in comparison with the conventional nucleating agents, sodium benzoate, and micrometric carbon/glass fibers.

EXPERIMENTAL

Materials

Commercial grade PET in pellet form was kindly provided by Yizheng Chemical Fiber Co. (Yizheng, China). The intrinsic viscosity of PET measured in phenol/1,1,2,2-tetrachloroethane (1 : 1 by mass) was 0.649 dL/g, corresponding to a viscosity average molecular weight of 47,500. Raw MWNTs prepared by catalytic chemical vapor deposition were purchased from Shenzhen Nanotech Port Co. (Shenzhen, China). Typical specifications of MWNTs according to the producer are as follows: diameters of 10∼20 nm and length of 5∼15 μm. MWNTs were purified by air oxidation to remove amorphous carbons and residual metal catalysts according to previous reported procedures.[21]

Chopped carbon fibers (Panex®33 carbon fiber, unsized, with diameter 7.2 μm, length 8.5 mm, tensile strength 3.8 GPa, and tensile modulus 228 GPa) were purchased from Zoltek (Bridgeton, MO). Carbon fibers were oxidized in air at 440°C for 30 min prior to experiment. Chopped E-glass fibers (ECS 301, sized, with diameter 10 μm, length 4.5 mm) were purchased from Chongqing Polycomp International Corp (Chongqing, China). As received from the manufacturer, glass fibers were coated with a proprietary silane-coupling agent, which was burned off in a furnace under air atmosphere at 500°C for 1 h. Commercial 2000-mesh talc powder was dried under vacuum. Sodium benzoate, phenol, 1,1,2,2-tetrachloroethane, trifluoroacetic acid, and dichloromethane were all analytical grade and used as received.

Preparation of PET composites

Prior to use, PET and fillers (MWNTs, carbon fibers, glass fibers, talc, and sodium benzoate) were dried under vacuum at 110°C for 12 h. The mass ratios of fillers versus PET were fixed as 0, 0.1%, 0.5%, 1%, 2.5%, and 5%.

PET composites were prepared by two methods: melt compounding and coagulation. Melt compounding was performed on a 2 cm^3-scale mixer (Mini-Max Molder CS-183MM, Custom Scientific Instruments Company, Cedar Knolls, NJ) at 265°C for 3 min. To ensure a complete compounding, melt-compounding process was repeated for three times. PET/MWNTs composites prepared by this method are denoted as M-PET/NT. Other composites of PET/carbon fibers, PET/glass fibers, PET/talc, and PET/sodium benzoate prepared by this melt-compounding method are denoted as PET/CF, PET/GF, PET/Talc, and PET/SB, respectively. Neat PET was also processed with the same procedures of melt compounding as reference, which was denoted as M-PET.

Coagulation method was performed by firstly dispersing MWNTs into PET solution in *o*-dichlorobenzene-phenol (1 : 1 by mass) and successively precipitating the dispersion with extensive methanol, as described previously.[21] The composites obtained from coagulation method are porous flocs. Using Mini-Max Molder CS-183MM machine, the composites were further melt-compounded for better homogeneity and injection-molded into bars with dimension of 50 × 12 × 1.5 mm^3. The resultant PET/MWNTs composites are denoted as C-PET/NT. Neat PET was also processed with the same procedures of coagulation as reference, which was denoted as C-PET.

All samples were dried under vacuum before experiment.

MWNTs dispersion state in M-PET/NT and C-PET/NT composites was observed on Leica Microsystems GmbH (Wetzlar, Germany) MPS-30 optical microscope. Thin films were obtained by first melting samples (about 5 mg) sandwiched by two glass slides at 280°C for 5 min on a temperature-controlled hot stage, and compressing the samples with a pair of tweezers, then quenching the samples to room temperature in air.

DSC characterization

DSC measurements were traced by Perkin–Elmer (Sheton, CT) DSC-7 under nitrogen atmosphere. Temperature was calibrated using indium (156.6°C) and zinc (419.5°C). Samples of about 7.0 mg were enclosed in aluminum pans, and an empty aluminum pan was used as reference. For regular DSC measurement, the procedures were as follows: heating from 35 to 280°C at the rate of 20°C/min, holding for 5 min, and then cooling to 100°C at the rate of 20°C/min. For isothermal analysis, samples were first held at 280°C for 5 min to erase thermal history, and then cooled to desired crystallization temperature T_c in the range of 215–245°C at the rate of 200°C/min. Samples were kept at T_c for sufficient time to allow DSC trace to level off. All tests were performed twice to ensure reproducibility.

Isothermal crystallization of thin films

Thin films were obtained by spin-casting a solution of PET or PET/MWNTs in CF_3COOH/CH_2Cl_2, and

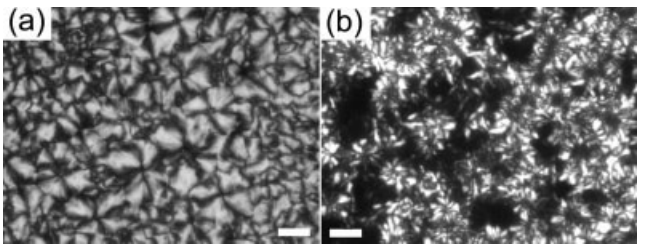

Figure 1 POM micrographs of spin-cast PET (a) and PET/MWNTs (0.1 wt % MWNTs) (b) films crystallized at 238°C for 120 min. The scale bars are equal to 10 μm.

then dried under vacuum at room temperature and protected with glass covers. Films were first melted at 280°C for 5 min on a temperature-controlled hot stage, and then cooled to desired temperature to carry out isothermal crystallization at the cooling rate of 10°C/min. The morphology of isothermal crystallized films was observed on Leica MPS-30 microscope with polarized light and JEOL (Tokyo, Japan) JEM-2010 transmission electron microscope. For POM, thin films were obtained from spin-casting 50 g/L solution on glass slides. For TEM, thin films were obtained from spin-casting 5 g/L solution on carbon-coated mica slides. The isothermal crystallized films were transferred to carbon-coated copper grids in deionized water, and then stained using ruthenium tetroxide (RuO_4) at room temperature for 30 min.[25]

Intrinsic viscosity measurement

Relative viscosities (η_r) of solutions (c = 0.5 g/dL) of PET, PET/SB, and C-PET/NT composites in the mixture of phenol and 1,1,2,2-tetrachloroethane (1:1 by mass) were determined using an Schott-Gerate viscometer at the temperature of (25 ± 0.1)°C. The solutions were filtered through sintered glass funnels with pore diameter of 2–5 μm before viscosity measurements. The intrinsic viscosity [η] was calculated using a single point determination method according to the following relationship:[26]

$$[\eta] = \frac{\sqrt{1 + 1.4(\eta_r - 1)} - 1}{0.7c} \quad (1)$$

The viscosity average molecular weight M_h was calculated using Mark-Houwink equation:

$$[\eta] = KM_\eta^\alpha \quad (2)$$

where K and α are Mark-Houwink constants. $K = 2.5 \times 10^{-4}$ dL/g, and α = 0.73.

RESULTS AND DISCUSSIONS

Morphology of heterogeneous nucleation of PET by MWNTs

As shown in POM micrographs (Fig. 1), isothermal crystallized PET/MWNTs thin films prepared from spin-casting method show an irregular spatial distribution of spherulites in comparison with pure PET samples prepared under same conditions. It is apparent that dense population of spherulitic crystallites surrounds MWNTs, while crystallite size is significantly reduced, and the shape become quite irregular. This is a direct consequence of an increase in the density of nucleating sites in the vicinity of MWNTs, which suggests heterogeneous nucleation of MWNTs on PET chains. TEM images confirm the nucleation action of MWNTs (Fig. 2). After RuO_4 staining of the amorphous regions of PET, it is found that MWNTs bundles locate in the center of crystal, and act as nuclei. The ''MWNTs boundles'' has been highlighted in a circle.

Isothermal crystallization kinetics and equilibrium melting point of C-PET/NT composites

Isothermal crystallization exotherms of C-PET/NT composites prepared from coagulation method are presented in Figure 3. The mass fraction crystallinity, X_t, is obtained from the exotherm area up to time t divided by the total exotherm, i.e.

$$X_t = \int_0^t (dH_t/dt)dt \Big/ \int_0^\infty (dH_c/dt)dt \quad (3)$$

where dH/dt is the heat flow rate. The shift of isotherms to right along the time axis with the increase of T_c indicates a decreasing crystallization rate.

Usually, crystallization half-time $t_{0.5}$, which is defined as the time when X_t is 0.5, or its reciprocal

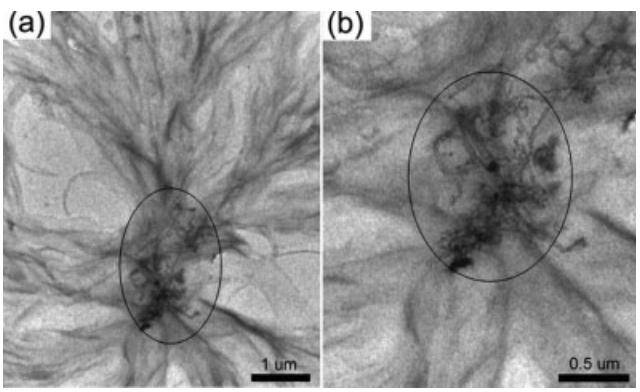

Figure 2 TEM micrographs of RuO_4-stained PET/MWNTs (0.1 wt % MWNTs) film crystallized at 228°C for 120 min in low and high magnifications. The ''MWNTs boundles'' has been highlighted in a circle.

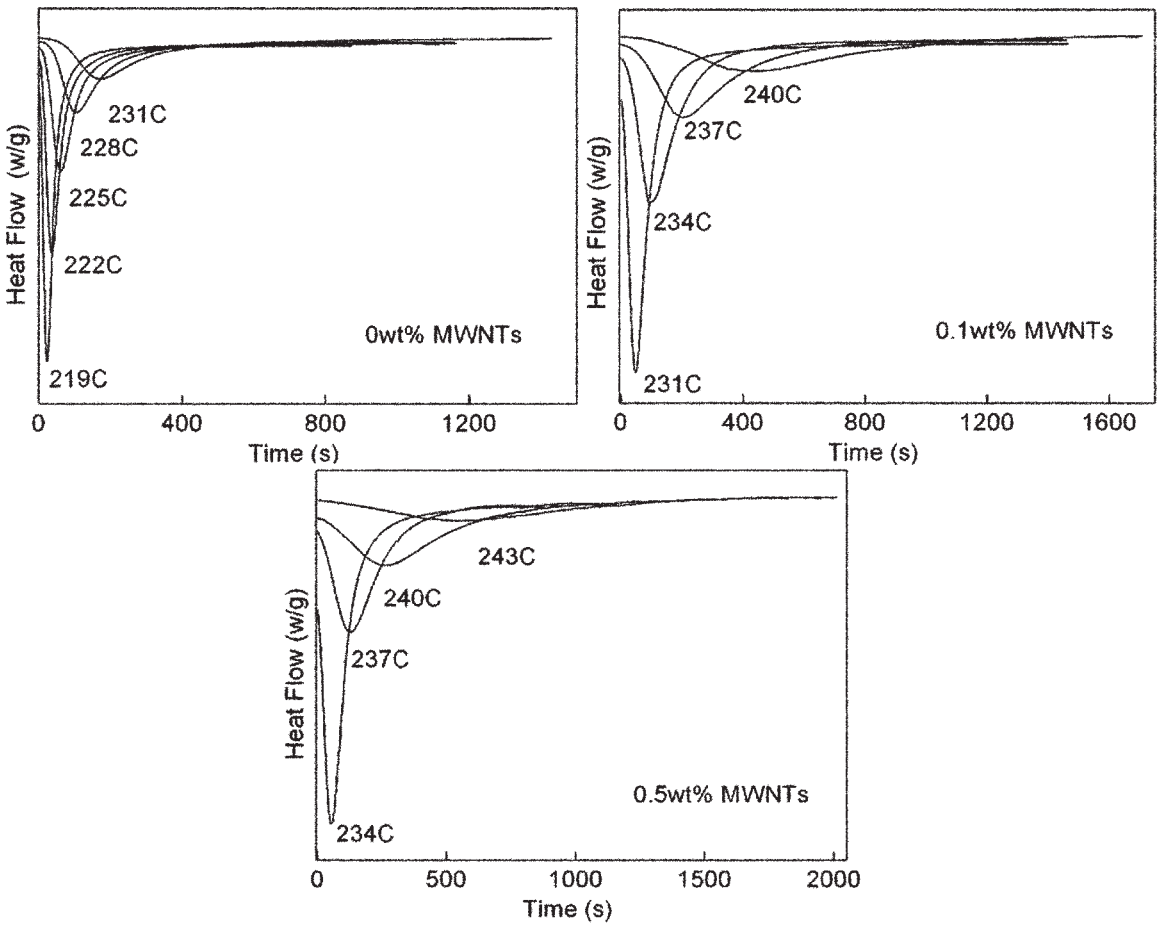

Figure 3 The DSC exotherms of isothermal crystallization of C-PET/NT composites with different loading of MWNTs under different crystallization temperature T_c.

$(t_{0.5})^{-1}$, is taken as a parameter of the crystallization rate of polymer. The dependence of $\ln(t_{0.5})^{-1}$ on T_c is shown in Figure 4. The crystallization rate of C-PET/NT composites is much larger compared with that of pure PET at the same T_c, and crystallization rate increases with the loading of MWNTs.

For analysis of crystallization kinetics for polymers, equilibrium melting point T_m^0 is an important parameter. According to the theory given by Hoffman and Weeks,[27] T_m^0 is related to the experimental melting point T_m and the isothermal crystallization temperature T_c with the following equation:

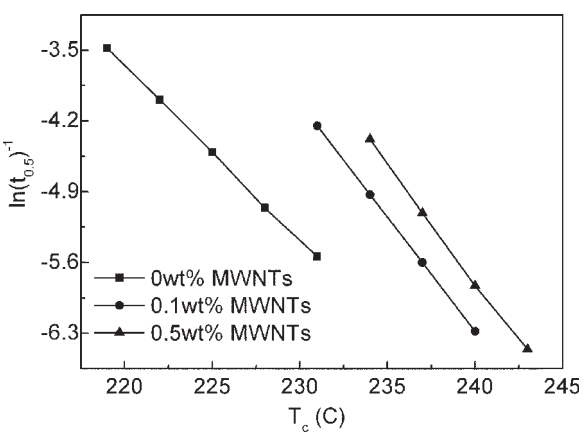

Figure 4 Plots of $\ln(t_{0.5})^{-1}$ versus T_c for PET and C-PET/NT composites.

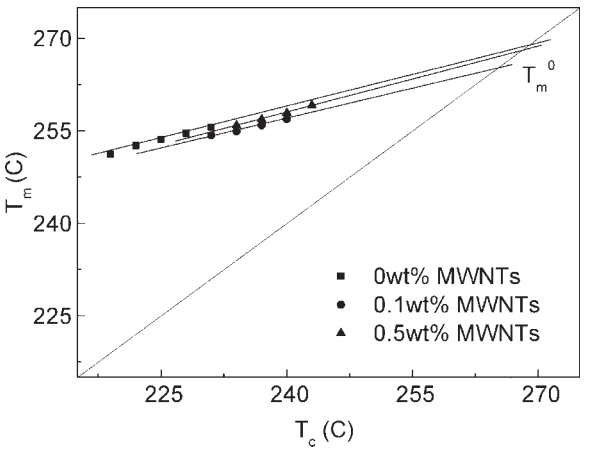

Figure 5 The determination of equilibrium melting point for PET and C-PET/NT composites.

TABLE I
Kinetics Parameters of Isothermal Crystallization for C-PET/NT Composites

MWNT (wt %)	T_c (°C)	$t_{0.5}$ (s)	$(t_{0.5})^{-1}$ (s^{-1})	$\ln(t_{0.5})^{-1}$	K (s^{-n})	n	T_m (°C)	T_m^0 (°C)
0	219	32.6	0.0307	−3.48	4.17×10^{-4}	2.13	251.4	269.0
	222	54.1	0.0185	−3.99	1.10×10^{-4}	2.20	252.6	
	225	90. 8	0.0110	−4.51	1.86×10^{-5}	2.34	253.5	
	228	158	0.00633	−5.06	3.45×10^{-6}	2.42	254.5	
	231	256	0.00391	−5.54	5.77×10^{-7}	2.53	255.6	
0.1	231	70.4	0.0142	−4.25	1.78×10^{-4}	1.94	254.9	265.3
	234	139	0.00719	−4.93	9.77×10^{-6}	2.27	255.9	
	237	272	0.00368	−5.60	8.91×10^{-7}	2.42	256.9	
	240	536	0.00186	−6.28	3.48×10^{-8}	2.68	257.9	
0.5	234	79.5	0.0128	−4.38	4.19×10^{-4}	1.70	255.8	268.3
	237	166	0.00602	−5.11	3.76×10^{-5}	1.92	256.9	
	240	340	0.00294	−5.83	1.57×10^{-5}	1.83	257.8	
	243	636	0.00157	−6.46	6.35×10^{-7}	2.15	259.4	

$$T_m = T_m^0(1 - 1/\gamma) + T_c/\gamma \quad (4)$$

where γ is the ratio of the thickness of grown crystallite to the thickness of critical crystalline nucleus.[28] Plotting T_m as a function of T_c, the extrapolation of T_m versus T_c to the line $T_m = T_c$ gives the value of T_m^0, as shown in Figure 5 and Table I.

To investigate the isothermal crystallization kinetics of C-PET/NT composites, the well-known Avrami equation[29] is employed:

$$\log[-\ln(1 - X_t)] = \log k + n \log t \quad (5)$$

where k is the overall kinetic constant, and n is the Avrami exponent, which is correlated to the nucleation mechanism and crystal growth dimension. The

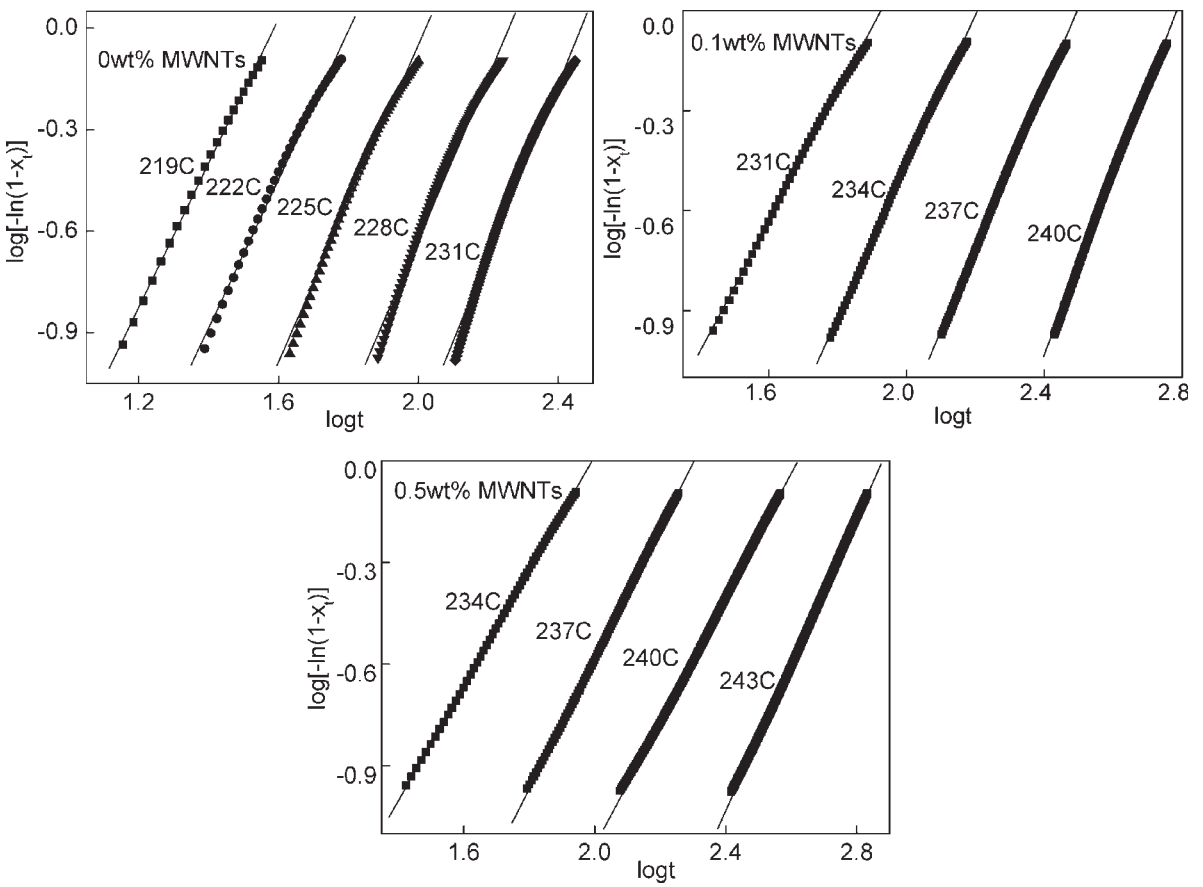

Figure 6 Avrami analysis of isothermal crystallization of C-PET/NT composites.

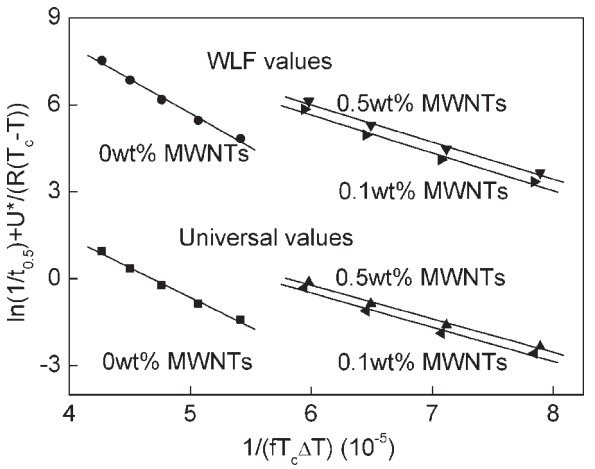

Figure 7 Plots of $\ln(1/t_{0.5}) + U^*/(R(T_c - T_\infty)$ versus $1/(fT_c\Delta T)$ by using WLF values and the universal values for PET and C-PET/NT composites.

isothermal crystallization of C-PET/NT composites is a typical two-stage process: primary crystallization and secondary crystallization. For brevity, we only analyze the primary stage (X_t = 10–55%). Figure 6 shows the plots of $\log[-\ln(1-X_t)]$ versus $\log t$ of C-PET/NT composites, from which n and k are determined, as presented in Table I. As could be seen, n increases with increasing T_c, but decreases with increasing loading of MWNTs from 0.1 to 0.5 wt %.

Lauritzen-Hoffman secondary nucleation theory

The reciprocal of $t_{0.5}$ could represent the crystallization rate of polymers:

$$G = (t_{0.5})^{-1} \tag{6}$$

According to the well-established Lauritzen-Hoffman (L-H) equation[30]:

$$G = G_0 \exp\left(-\frac{U^*}{R(T_c - T_\infty)}\right) \exp\left(-\frac{k_g}{fT_c\Delta T}\right) \tag{7}$$

$$(t_{0.5})^{-1}[(t_{0.5})_0]^{-1} \exp\left(-\frac{U^*}{R(T_c - T_\infty)}\right) \exp\left(-\frac{k_g}{fT_c\Delta T}\right) \tag{8}$$

where G_0 is a preexponential factor containing quantities not strongly dependent on temperature, U^* is the activation energy for the transport of polymer segments to the crystallization site, R is the gas constant, ΔT is the degree of supercooling ($\Delta T = T_m^0 - T_c$), T_m^0 is the equilibrium melting temperature, $f = 2T_c/(T_c + T_m^0)$ is the correction factor accounting for the variation in ΔH_m^0 (the fusion heat of perfect crystal) with temperature. T_∞ ($T_\infty = T_g - C$) is the temperature where the cessation of long-range molecular motion is expected, and T_∞ is often taken to be either $\sim$30 or 51.6 K below T_g, glass-transition temperature (i.e., $T_g \approx 78^\circ$C for PET).

For a given growth regime, the constant k_g can be defined as

$$k_g = \frac{4\sigma\sigma_e b_0 T_m^0}{k_b \Delta H_m^0} \tag{9}$$

where k_b is the Boltzmann's constant, b_0 is the thickness of a monomolecular layer, σ and σ_e are the lateral surface free energy, and the fold surface free energy during nucleation process, respectively.

Medellin-Rodriguez et al.[31] discussed the applicability of L-H equation to polymers. They employed the empirical ''universal'' values of U^* = 6284 J/mol and $T_\infty = T_g - 30$ K, and the Williams-Landel-Ferry values[32] of U^* = 17,640 J/mol and $T_\infty = T_g - 51.6$ K. For isothermal crystallization of PET, b_0, σ, and ΔH_m^0 are taken as 0.595 nm, 1.09×10^{-2} J/m^2, and 2.1×10^8 J/m^3, respectively.[14] Thus, the dependence of $\ln(1/t_{0.5}) + U^*/(R(T_c - T_\infty))$ on $1/(fT_c\Delta T)$ for C-PET/NT composites is plotted in Figure 7 and the resulted k_g and σ_e values are listed in Table II. A good nucleating agent would provide surfaces of low free energy. The smaller is the free energy, the smaller is the work required in folding polymers chains. σ_e for MWNTs nucleated PET is just half of pure PET, meaning that MWNTs are efficient nucleating agents for PET.

Influence of MWNTs dispersion state on nucleating ability

MWNTs dispersion state is a crucial factor to the properties of target composites. Our previous

TABLE II
Results Determined by L-H Equation Based on Different Parameters for C-PET/NT Composites

MWNTs (wt %)	K_g (K^{-2})[a]	σ_e[a] (J m^{-2})	K_g (K^{-2})[b]	σ_e[b] (J m^{-2})
0	2.05×10^5 (0.996)[c]	0.0428	2.36×10^5 (0.996)	0.0493
0.1	1.18×10^5 (0.992)	0.0247	1.31×10^5 (0.992)	0.0272
0.5	1.16×10^5 (0.996)	0.0241	1.28×10^5 (0.996)	0.0267

[a] Values are obtained from universal values.
[b] Values are from WLF values.
[c] Values in parentheses represent correlation coefficient (R) for the fitted straight lines.

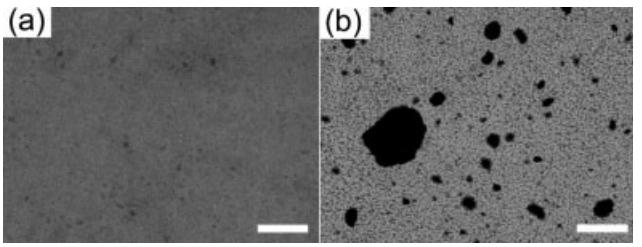

Figure 8 Optical micrographs of C-PET/NT (a) and M-PET/NT (b) composites. The loading of MWNTs is 0.5 wt %, and the scale bars are equal to 50 μm.

results[21] have shown that coagulation method produces homogeneous PET/MWNTs composites. Here, we characterize MWNTs dispersion state with optical micrographs. There are few agglomerates of MWNTs in the coagulated C-PET/MWNTs composites [Fig. 8(a)]. In contrast, numerous black spots, which are responsible to MWNTs agglomerates, appear in the melt compounded M-PET/MWNTs composites [Fig. 8(b)]. The poor dispersion indicates that there is macrophase separation in M-PET/NT composites.

The effect of MWNTs dispersion state on crystallization characteristics of PET matrix has been analyzed using regular DSC experiments. DSC cooling scans of PET/MWNTs composites are shown in Figure 9. Composite samples exhibit crystallization exotherms earlier than pure PET. The dependence of maximum crystallization rate temperature T_{peak} on mass ratio of MWNTs is plotted in Figure 10. Given MWNTs loading of 2.5 wt %, T_{peak} increases 11.7°C for C-PET/NT composites in comparison with the reference C-PET sample, and 7.9°C for M-PET/NT composites in comparison with the reference M-PET sample. This indicates that nucleation effect is greatly enhanced when homogeneous MWNTs dispersion achieved.

Nucleating ability comparison between MWNTs and commercial nucleating agents and fibers

Sodium benzoate and talc are commercial nucleating agents for PET, while carbon fibers and glass fibers are widely used as reinforcing fillers for resins. In comparison with PET/MWNTs composites, PET/SB, PET/CF, PET/GF, and PET/talc composites were prepared by melt compounding. DSC cooling scans of melt-compounded PET/SB, PET/CF, PET/GF, and PET/talc composites are shown in Figure 11. As presented in Figure 11, all composite samples exhibit crystallization exotherms earlier than their reference M-PET sample prepared under the same melt-compounding conditions as composite samples. The dependence of T_{peak} on various mass ratios of different fillers is plotted in Figure 12. In comparison with reference M-PET sample prepared under the same conditions as composite samples, at the filler loading of 2.5 wt %, T_{peak} increases 15.6°C for PET/SB composites, 7.9°C for M-PET/NT composites, 5.6°C for PET/talc composites, 2.3°C for PET/carbon fibers composites, and 1.9°C for PET/glass fibers composites. This indicates that sodium benzoate possesses the best nucleating ability to PET among them. The nucleating ability sequence of fillers is as followed: sodium benzoate>MWNTs>talc>carbon fibers≈glass fibers.

The thermal degradation of polymers has a strong influence on their crystallization. Since C-PET/NT composites and PET/SB composites give most prominent nucleating effect, we measured the molecular weight of PET of these two series with the viscosity method. Although the solutions were filtered before viscosity measurements, it should be noted that the filtrate was still black for C-PET/NT composites, indicating that some MWNTs could not be completely removed by the filtration process. Moreover, sodium benzoate is soluble in PET solvent, so it may also have some influence on measurement results.

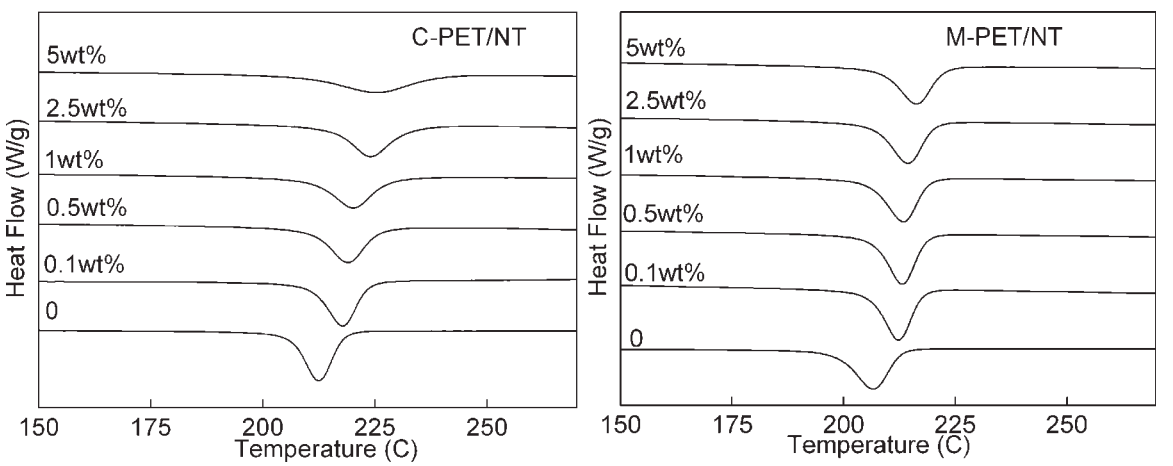

Figure 9 DSC cooling scans of C-PET/NT, M-PET/NT composites.

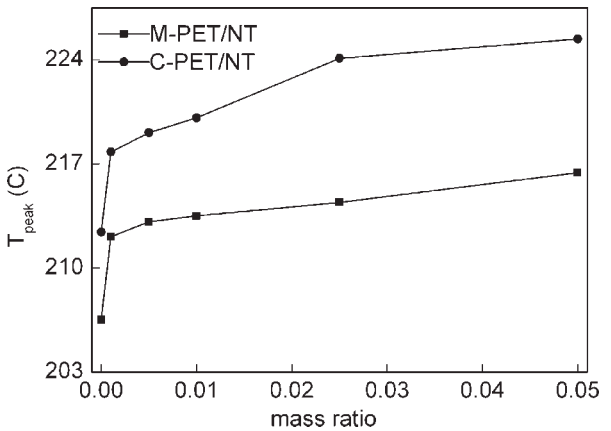

Figure 10 T_{peak} versus mass ratio of fillers of C-PET/NT, M-PET/NT composites.

However, the influence of MWNTs or sodium benzoate on measurement results should be insignificant due to the low concentration in solution (less than 200 ppm in solution). To clarify the effect of residual MWNTs or sodium benzoate on the viscosity measurements, we did measure the viscosity of the solutions of as-received PET sample in the presence of MWNTs and sodium benzoate (''PET + MWNTs'' and ''PET + sodium benzoate'' in Table III) under the same viscosity measuring process. ''PET + sodium benzoate'' is a solution of as-received PET sample in the presence of sodium benzoate with the same concentration as that of PET/SB (5 wt %) composites, and ''PET + MWNTs'' is a solution of as-received PET sample in the presence of MWNTs with the same concentration as that of C-PET/NT (5 wt %) composites. We found that neither MWNTs nor sodium benzoate had significant influence on the viscosity measurements (Table III).

PET/SB composites have initiated great decrease in the molecular weight of PET (Table IV). For PET/SB, the molecular weight drop of PET (0 wt % of filler) from 47.5 kg/mol (Table III) to 35.3 kg/mol (Table IV) is mainly due to the thermal degradation in melt mixing process. 5 wt % sodium benzoate induces a reduction of viscosity average molecular weight of PET as large as 45%. In fact, the color of PET/SB composites become yellow with the increasing amount of sodium benzoate, indicating that PET/SB composites have experienced severe degradation with high loading of sodium benzoate during

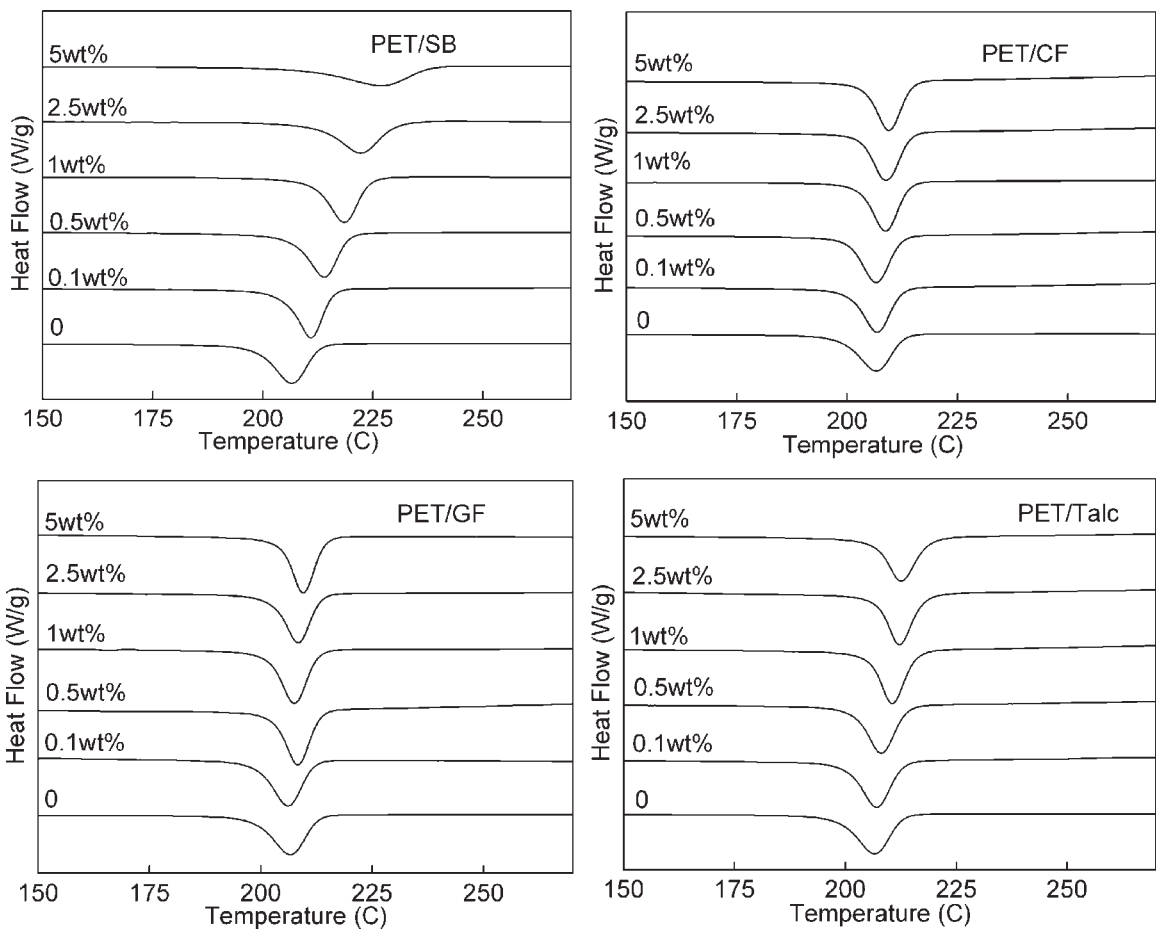

Figure 11 DSC cooling scans of PET/SB, PET/CF, PET/GF, and PET/talc composites.

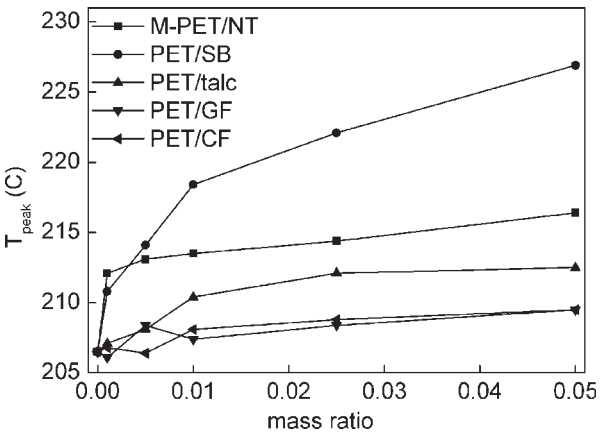

Figure 12 T_{peak} versus mass ratio of fillers of various composites including PET/SB, M-PET/NT, PET/CF, PET/GF, PET/talc.

preparation. The following reaction between metal salts and PET during melt processing was proposed by Garcia:[17]

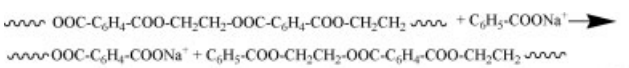

(10)

This reaction points out that PET nucleation in the presence of effective metal salts such as sodium benzoate is a chemical nucleation process: a reaction between polymer and an organic salt leads to the formation of ionic chain ends; the resulting ionic clusters are thought to precipitate and form the nuclei. It also explains the drop in molecular weight of PET in our experimental results with the increasing content of sodium benzoate.

On the other hand, MWNTs influence little on the molecular weight of PET in C-PET/MWNTs composites (Table IV). For C-PET/NT, the molecular weight drop of PET (0 wt % of filler) from 47.5 kg/mol (Table III) to 34.3 kg/mol (Table IV) is mainly due to the thermal degradation in melt processing process after coagulation. Li et al.[33] have reported nano-hybrid shish-kebab structures from solution crystallization of polymers in the presence of CNTs, which is CNTs periodically decorated with polymer lamellar crystals, and they have proposed a ''size-dependent soft epitaxy'' mechanism. In melt crystallization, the viscosity is larger than solution for magnitudes, so polymer chains might not have enough time and energy to pattern themselves onto MWNTs, therefore regular spherulites morphology is observed. MWNTs nucleate PET through ''particle effect,'' which does not affect the molecular weight of PET. Because of their high aspect ratio, small diameter and uniform dispersion, nucleation density of MWNTs is large enough to excel talc, which nucleates PET through lattice matching epitaxial mechanism.[20]

TABLE III
Viscosity Average Molecular Weight of As-Received PET, PET + Sodium Benzoate, and PET + MWNTs

Samples	PET	PET + sodium benzoate	PET + MWNTs
M_η (kg/mol)	47.5	48.4	47.4

CONCLUSIONS

The crystallization behavior of PET/MWNTs composites has been investigated with POM, TEM and DSC. In comparison with pure PET, POM images show that spherulites size of PET/MWNTs composites is significantly reduced, and the shape becomes quite irregular. TEM images show that MWNTs bundles locate in the center of crystal and act as nuclei. To make a detailed analysis of the crystallization behavior of PET/MWNTs composites, the renowned Avrami equation and Lauritzen-Hoffman secondary nucleation theory have been employed. The value of Avrami exponent n has a dependence on the loading of MWNTs. Higher loading of MWNTs decreases the value of n. The crystallization rate of PET increases exponentially with the addition of MWNTs. The fold surface free energy during nucleation process for MWNTs nucleated PET is just half of pure PET, suggesting that MWNTs are efficient nucleating agents for PET.

MWNTs dispersion state has a significant influence on their nucleating effect. Nucleation effect is significantly enhanced when homogeneous MWNTs dispersion achieved. The nucleating ability of MWNTs is compared with commercial nucleating agents and fibers, and the sequence is as followed: sodium benzoate>MWNTs>talc>carbon fibers≈glass fiber. PET nucleation in the presence of sodium benzoate is a chemical nucleation process, which causes severe degradation of PET. MWNTs nucleate

TABLE IV
Viscosity Average Molecular Weight of PET/SB and C-PET/NT Composites

Samples	PET/SB						C-PET/NT					
Mass ratio of filler (%)	0	0.1	0.5	1	2.5	5	0	0.1	0.5	1	2	5
M_η (kg/mol)	35.3	33.8	33.3	27.7	22.8	19.4	34.3	34.2	33.9	34.5	33.6	34.4

PET through ''particle effect,'' which does not affect the molecular weight of PET.

References

1. Coleman, J. N.; Khan, U.; Gun'ko, Y. K. Adv Mater 2006, 18, 1.
2. Kharchenko, S. B.; Douglas, J. F.; Obrzut, J.; Grulke, E. A.; Migler, K. B. Nat Mater 2004, 3, 564.
3. Kashiwagi, T.; Grulke, E.; Hilding, J.; Harris, R.; Awad, W.; Douglas, J. Macromol Rapid Commun 2002, 23, 761.
4. Zhang, W. D.; Shen, L.; Phang, I. Y.; Liu, T. Macromolecules 2004, 37, 256.
5. Meincke, O.; Kaempfer, D.; Weickmann, H.; Friedrich, C.; Vathauer, M.; Warth, H. Polymer 2004, 45, 739.
6. Pötschke, P.; Fornes, T. D.; Paul, D. R. Polymer 2002, 43, 3247.
7. Du, F.; Fisher, J. E.; Winey, K. I. J Polym Sci Part B: Polym Phys 2003, 41, 3333.
8. Kogonemaru, A.; Bin, Y.; Agari, Y.; Matsuo, M. Adv Funct Mater 2004, 14, 842.
9. Sabba, Y.; Thomas, E. L. Macromolecules 2004, 37, 4815.
10. Nogales, A.; Broza, G.; Roslaniec, Z.; Schulte, K.; Sÿics, I.; Hsiao, B. S.; Sanz, A.; García-Gutiérrez, M. C.; Rueda, D. R.; Domingo, C.; Ezquerra, T. A. Macromolecules 2004, 37, 7669.
11. Zhao, C. G.; Hu, G. J.; Justice, R.; Schaefer, D. W.; Zhang, S. M.; Yang, M. S.; Han, C. C. Polymer 2005, 46, 5125.
12. Regev, O.; ElKati, P. N. B.; Loos, J.; Koning, C. E. Adv Mater 2004, 16, 248.
13. Xia, H.; Wang, Q.; Li, K.; Hu, G.-H. J Appl Polym Sci 2004, 93, 378.
14. Lu, X. F.; Hay, J. N. Polymer 2002, 41, 9423.
15. Ke, Y. C.; Long, C. F.; Qi, Z. N. J Appl Polym Sci 1999, 71, 1139.
16. Sorrentino, L.; Iannace, S.; Di maio, E.; Acierno, D. J Polym Sci Part B: Polym Phys 2005, 43, 1966.
17. Garcia, D. J Polym Sci Polym Phys Ed 1984, 22, 2063.
18. Xanthos, M.; Baltzis, B. C.; Hsu, P. P. J Appl Polym Sci 1997, 64, 1423.
19. Martínez-Vázquez, D. G.; Medellín-Rodríguez, F. J.; Phillips, P. J.; Sanchez-Valdes, S. J Appl Polym Sci 2003, 88, 360.
20. Haubruge, H. G.; Daussin, R.; Jonas, A. M.; Legras, R. Macromolecules 2003, 36, 4452.
21. Hu, G. J.; Zhao, C. G.; Zhang, S. M.; Yang, M. S.; Wang, Z. G. Polymer 2006, 47, 480.
22. Assouline, E.; Lustiger, A.; Barber, A. H.; Cooper, C. A.; Klein, E.; Wachtel, E.; Wagner, H. D. J Polym Sci Part B: Polym Phys 2003, 41, 520.
23. Probst, O.; Moore, E. M.; Resasco, D. E.; Grady, B. P. Polymer 2004, 45, 4437.
24. Phang, I. Y.; Ma, J. H.; Shen, L.; Liu, T. X.; Zhang, W. D. Polym Int 2006, 55, 71.
25. Haubruge, H. G.; Jonas, A. M.; Legras, R. Polymer 2003, 44, 3229.
26. Hergenrother, W. L.; Nelson, C. J. J Polym Sci Polym Chem Ed 1974, 12, 2905.
27. Hoffman, J. D.; Weeks, J. J. J Res Natl Bur Stand Sect A 1962, 66, 13.
28. Alamo, R. G.; Viers, B. D.; Mandelkern, L. Macromolecules 1995, 28, 3205.
29. Avrami, M. J Chem Phys 1940, 8, 212.
30. Hoffman, J. D.; Davis, G. T.; Lauritzen, J. I., Jr. In Treatise in Solid State Chemistry; Hannay, N. B., Ed.; Plenum Press: New York, 1976; Vol. 3, Ch. 7, p 497.
31. Medellin-Rodriguez, F. J.; Phillips, P. J; Lin, J. S. Macromolecules 1995, 28, 7744.
32. Williams, M. L.; Landel, R. F.; Ferry, J D. J Am Chem Soc 1955, 77, 3701.
33. Li, L. Y.; Li, C. Y.; Ni, C. Y. J Am Chem Soc 2006, 128, 1692.